A SOFT SWITCHING CONSTANT FREQUENCY PWM DC/DC CONVERTER WITH LOW SWITCH STRESS AND WIDE LINEARITY

In-Dong Kim, Eui-Cheol Nho and Gyu-Hyeong Cho

Dept. of Electrical Engineering,
Korea Advanced Institute of Science and Technology
P.O.Box 150 Chongryang, Seoul 130-650, Korea (FAX : Seoul(2) 960-2103)

ABSTRACT

A new zero voltage switching (ZVS) DC/DC converter which operates on constant frequency and has wide linearity is proposed. ZVS operations are achieved not only for the primary switches but also for the secondary rectifier diodes to reduce the switch stresses and losses. The proposed converter also overcomes the other shortcomings of the conventional resonant DC/DC converters such as high VA ratings of devices and passive components, load-dependent DC characteristics, etc.

I. INTRODUCTION

A number of DC/DC converters employing either zero voltage or zero current high frequency switching operation have been studied extensively. Resonant type converters and quasi resonant type converters [1-3] can operate at high frequency with low switching loss and low EMI. Thus these converters have merits such as reduced size and weight of the filters and isolation transformers. However, they also have several well-known problems such as high VA ratings of devices and components, variable switching frequency, load dependent DC characteristics and complex control. The other converters which are partially resonant only during switching transients appear in literatures [4,5]. These partial resonant converters use reactive elements or capacitive snubbers to shape the switching trajectory of the device to realize zero voltage switching. The reactive elements are not involved in primary power transfer but act as snubbing function only. Thus, VA ratings of the elements and their dissipations due to effective series resistance (ESR) are very low compared with those of the resonant and quasi-resonant converters. However, these converter should be designed considering large ripple current handling capabilities at the output capacitor and high current stresses in the devices because the resonant inductors which act as energy transfer elements have almost triangular current waveforms. In addition, the DC conversion-ratio characteristics are non-linear and load-dependent although these converters operate at constant switching frequency by utilizing the phase-shift control technique.

In this paper, a new zero voltage switching PWM DC/DC converter which overcome the shortcomings of the conventional resonant DC/DC converters as mentioned above is proposed. ZVS operations are achieved not only for the primary switches but also for the secondary rectifier diodes to reduce the switch stresses and losses. Besides, the voltage and current stresses of the devices and components in the proposed converter are reduced and always clamped to the supply voltage V_S and the output current I_O, respectively.

II. PRE-PROPOSED CONVERTER

The basic configuration of the primitive type is full bridge one with output filter L_O as shown in Fig. 1. Each pole is composed of series connected two switches to which resonant capacitors and diodes are connected in parallel. The main role ot resonant inductor L_r and the resonant capacitors is to provide the zero voltage switching condition. The filter inductor L_o is large enough to maintain almost constant output current. The typical waveforms of the pre-proposed converter are represented as shown in Fig. 2. In appearance, the pre-proposed scheme looks like the partial-resonant type converter in a sense that resonant elements L_r, $C_r(C_1-C_4)$ resonate partially only for the duration of switching transient so as to ensure zero voltage switching condition. However, the proposed converter not only gives the partial-resonant operation but also provides the particular operation of either series-connection mode or decoupled mode between two inductors L_r, L_o.

Fig. 3 (a) represents the equivalent circuit of the proposed converter during a time-interval (from mode 2 to 3) where both inductors are series-connected and thus resonant inductor current i_{Lr} remains clamped to the output filter inductor current I_O :

$$i_{Lr}(t) = I_O . \tag{1}$$

On the other hand, during subsequent time-interval (from mode 4 to 1), the proposed converter is divided into two isolated equivalent circuits by decoupling two inductors through short-circuit of diode bridge as shown in Fig. 3 (b). In this interval, the output current

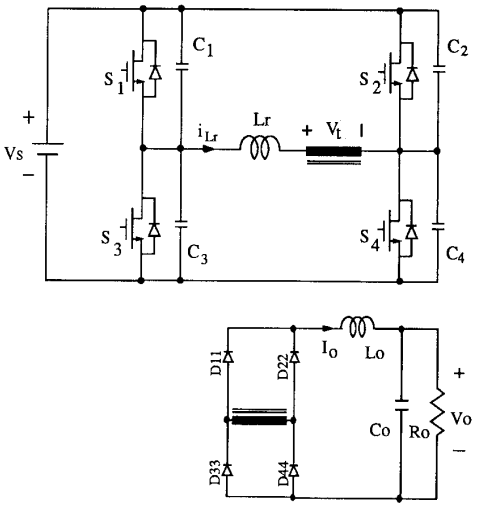

Fig. 1 Pre-proposed zero-voltage-switching PWM DC/DC converter

087942-600-4/90/1100-0875$01.00 © 1990 IEEE

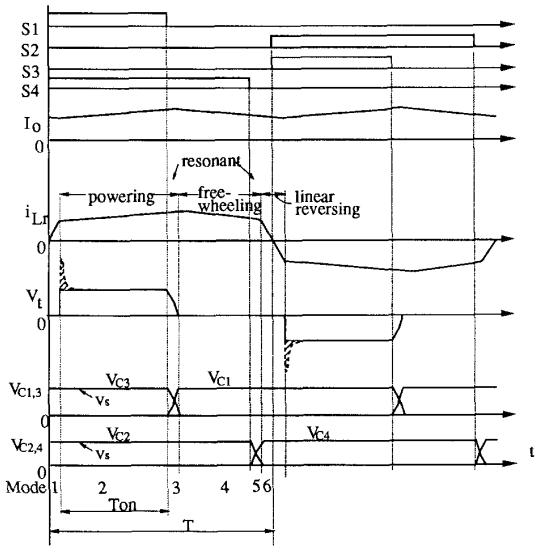

Fig. 2 Typical waveforms of pre-proposed converter (the dotted parts of waveform V_t are the case of considering reverse recovery of off-going output diodes).

I_O is kept almost constant by freewheeling through shorted diodes and load R_o whereas the resonant current i_{Lr} becomes partially resonant and linearly decreases via zero to the output current I_O, or

$$|i_{Lr}(t)| < I_O . \tag{2}$$

When the resonant current i_{Lr} reaches to the output current I_O, both inductors are series-connected again and thus the next cycle begins. Therefore, the current stresses of devices and components are low and always clamped to the output current I_O.

When the two inductors are series-connected power is transferred from source to load whereas there is no power transfer when the inductors are decoupled. For that reason, the power transfer mechanism of the proposed converter can be represented as powering and freewheeling operation similar to that of switched mode PWM converter. The output power can be regulated by varying the duty ratio of powering and freewheeling intervals. The duty ratio control or pulse width modulation control enables constant switching operation and results in linear and load-independent DC characteristics. Even though this primitive type converter provides many good features as mentioned above, it severely suffers from reverse recovery problem as typically encountered in many power converters.

III. RECOVERY PROBLEM IN THE OUTPUT DIODES

Many nontrivial limitations of the diodes are caused by the property that is universal in all of the silicon devices. The property is excess stored charge needed to sustain forward current flowing. The most important diode limitation that arises due to the stored charge is reverse recovery. The diode reverse recovery phenomena in the power converters have been among the most troublesome and acute problems faced by converter designers. The pre-proposed converter also suffer from the reverse recovery phenomenon during transition transients between mode-1 and mode-2. Fig. 4 shows the equivalent circuit and corresponding waveforms during reverse recovery. During mode 1 $[t_0, t_1]$, the

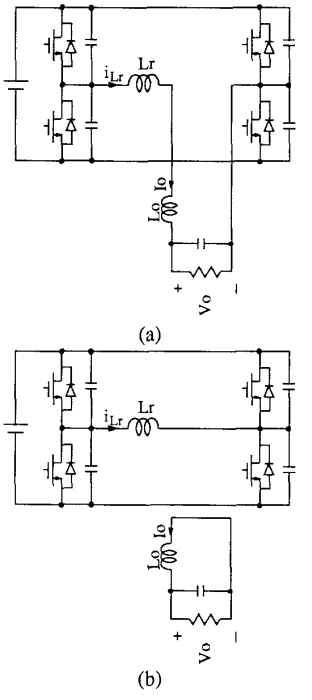

Fig. 3 Equivalent circuits (a) series-connection of L_r and L_O (from mode 2 to mode 3), (b) seperation (from mode 4 to mode 1).

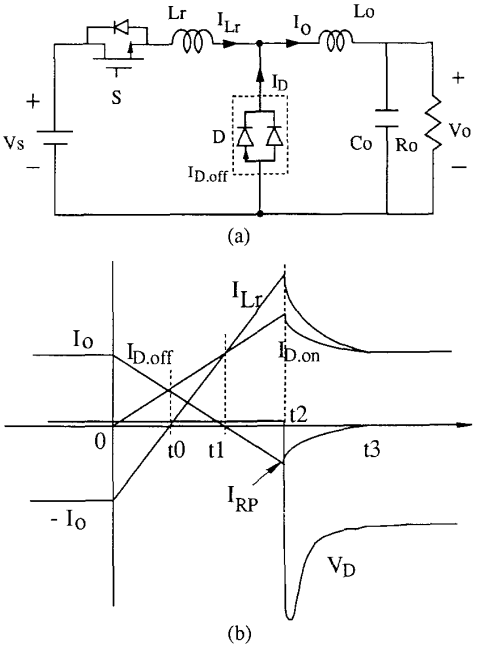

Fig. 4 Reverse recovery phenomena of the pre-proposed converter (a) equivalent circuit during reverse recovery, (b) charcateristic waveforms ($i_{D,on}$: on-comming diode current, $i_{D,off}$: off-going diode current).

current through the off-going output diode D22, D33 are linearly decreased while the resonant inductor current is increased from zero to I_O. At time instant t_1, diode reverse recovery process is initiated and thus the diode current I_d builds up reversely at a rate limited by a resonant inductor L_r, or

$$\frac{dI_d}{dt} \approx \frac{V_S}{L_r} \tag{3}$$

until the stored charges of the output diodes are completely removed. The peak reverse diode current is found to be

$$I_{RP} = \sqrt{\frac{V_S I_O \tau_S}{L_r}} \tag{4}$$

where τ_S is the storage time constant of the diode. This process should store excess energy in the resonant inductor and impose peak current stress $(I_O + I_{RP})$ on the main switch. Subsequent diode snap-off between t_2 and t_3 causes substantially large voltage spike across the off-going output diodes, or

$$V_{spike} = V_S - L_r \frac{dI_d}{dt} \tag{5}$$

and results in very large dissipations in the output diodes given by

$$P_{loss} = \frac{1}{T_s}\int_{t_2}^{t_3} V_{spike} I_d \, dt \tag{6}$$

$$= V_S Q_j f_S + \frac{L_S}{2} I_{RP}^2 f_S \tag{7}$$

where f_S is the switching frequency and Q_j is the reverse recovery charge during snap-off.

These problems limit the maximum switching frequency of the converter and result in substantial reduction of system efficiency and reliability.

IV. PROPOSED CONVERTER

Usually the reverse recovery problem of output diodes D_{11}-D_{44} is inevitable in the transformer coupled inductive filter circuits such as the pre-proposed converter and brings about severely large voltage spikes across the diodes. Thus, the high voltage ratings of the diodes are required and the switching loss becomes high. These problems are eliminated by providing zero voltage switching of the output bridge diodes. Fig. 5 shows the proposed converter having an auxiliary circuit. The auxiliary circuit which consists of C_{rr} and diode bridge $(D_{a1}-D_{a4})$ gives the solution for the reverse recovery problem of the output bridge diodes by connecting a capacitor C_{rr} to the two terminals of another winding of the isolation transformer whose turn-ratio is n_1 to n_3. The capacitor voltage increases resonantly and is clamped finally to supply voltage V_S owing to the auxiliary bridge diodes $D_{a1}-D_{a4}$. Consequently the combination of the third isolation winding, L_r, C_{rr} and auxiliary diode bridge returns the reverse recovery energy of the output diodes and provides zero voltage switching to the diodes. The power rating of the auxiliary bridge diodes is very low because they handle the excess stored energy in the inductor L_r. It should also be noted that the proposed converter with auxiliary circuit does not disturb the good features of the primitive type at all.

Power transfer in the proposed converter is done basically through the powering and freewheeling intervals as in the conventional PWM dc/dc converter having constant switching frequency. Resonant capacitors $C_r(C_1$-$C_4)$ and C_{rr} are used to ensure the zero voltage switching of all of the devices and charged and discharged only during switching transient intervals with resonant inductor L_r. Because the capacitors C_r and C_{rr} are not involved in the primary power transfer, VA ratings of the capacitors are significantly reduced compared with those of the resonant type converter. The peak resonant inductor current i_{Lr} is limited to the output current

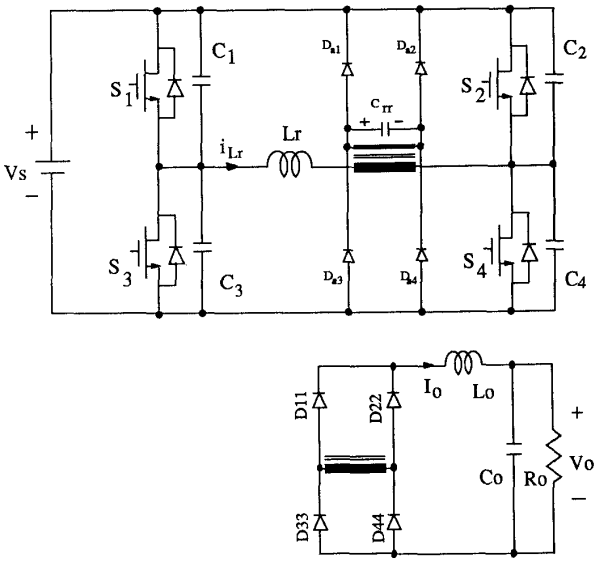

Fig. 5 Proposed zero-voltage-switching PWM DC/DC converter.

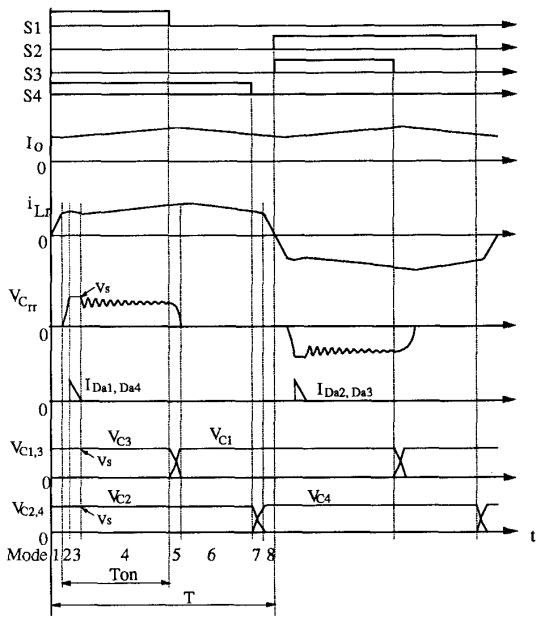

Fig. 6 Typical waveforms of proposed converter.

I_o during the powering interval (modes 2-5) because resonant inductor L_r and output filter inductor L_o effectively works in series. The inductance value L_o is chosen to be large enough than L_r to be replaced by a current source I_O. During the next freewheeling interval followed by the powering one, the two inductors are effectively separated through short-circuiting of the output bridge diodes and thus the remaining resonant inductor current i_{Lr} freewheels through L_r, $S_4(S_2)$ and parallel-connected diode of $S_3(S_1)$, and the output inductor current freewheels through the short-circuited output bridge diodes. This operation continues even when the inductor current i_{Lr} changes its polarity by turning off $S_4(S_2)$ and turning on $S_2(S_4)$ until the current i_{Lr} reaches the freewheeling output current I_O. Consequently, through one cycle switching operation, the resonant inductor current i_{Lr} is always limited to the output

current I_o and thus the current stresses of the devices become very low compared to that of the resonant type converter. Zero voltage switching of S_4, $S_2(S_3, S_1)$ is achieved because the voltage across S_4, $S_2(S_3, S_1)$ rises with finite slope due to the partial resonant operation of L_r and $2C_r(C_4+C_2$ or $C_3+C_1)$.

V. OPERATION MODES

The overall operation of the proposed converter can be divided into powering (mode 4), resonant (mode 2, 5, 7), freewheeling (mode 6), linear increasing and decreasing (mode 1, 8) modes according to the inductor current waveform i_{Lr}. The output capacitor C_O is assumed to be sufficiently large to be replaced by voltage source V_O. The isolation transformer turn-ratio between the first and the second windings is assumed one-to-one and another turn-ratio between the first and the third winding (connected to the auxiliary circuit) is assumed to be $a=n_1/n_3$. The typical waveforms and the corresponding topological mode diagrams are shown in Fig. 6 and 7, respectively.

(I). Mode 1 (*linear increasing*) : This mode occurs with all output bridge diodes conducted, thereby effectively decouples the resonant circuit and output circuit. Thus the resonant inductor current increases linearly by the supply voltage and the output current I_O freewheels through the short-circuited output bridge diodes, that is,

$$i_{Lr}(t)=\frac{V_S}{L_r}t, \tag{8}$$

$$I_O(t)=I_O(t_0)-\frac{V_O}{L_O}t. \tag{9}$$

(II). Mode 2 (*resonant*) : As soon as the resonant inductor current i_{Lr} reaches the peak current (I_O+I_{RP}), only two output diodes remain conducting state, and the others are turned off under zero voltage switching condition provided by the resonant operation of L_r and C_{rr}. The zero voltage switching operation eliminates large voltage spikes and reverse recovery losses of off-going output diodes. Then the capacitor voltage V_{Crr} and the resonant inductor current i_{Lr} can be found to be

$$V_{Crr}=\frac{n_3}{n_1}[V_S+\sqrt{(I_{RP}Z_{rr})^2+V_S^2}\ \sin(\omega_{rr}t-\tan^{-1}\frac{V_S}{I_{RP}Z_{rr}})] \tag{10}$$

$$i_{Lr}=I_O+\sqrt{I_{RP}^2+(V_S/Z_{rr})^2}\ \cos(\omega_{rr}t-\tan^{-1}\frac{V_S}{I_{RP}Z_{rr}}) \tag{11}$$

$$Z_{rr}=\sqrt{L_ra^2/C_{rr}}. \tag{12}$$

(III). Mode 3 (*clamping*) : The resonantly increasing capacitor voltage V_{Crr} is clamped to V_S and the excess stored energy in the resonant inductor L_r is delivered to the power supply V_S. Thus the resonant inductor current i_{Lr} decreases linearly toward I_O, or

$$\frac{di_{Lr}}{dt}=V_S(1-a)-2V_{FET.on}-2aV_{D.on}\ . \tag{13}$$

(IV). Mode 4 (*powering*) : In this mode, power is transferred from source to load similar to the powering stage of the conventional switched mode PWM converter :

$$I_O(t)=I_O(t_3)+\frac{V_S}{L_r+L_O}t \tag{14}$$

$$i_{Lr}(t)=I_O+\frac{V_S(1-a)}{Z_{rr}}\sin(\omega_{rr}t). \tag{15}$$

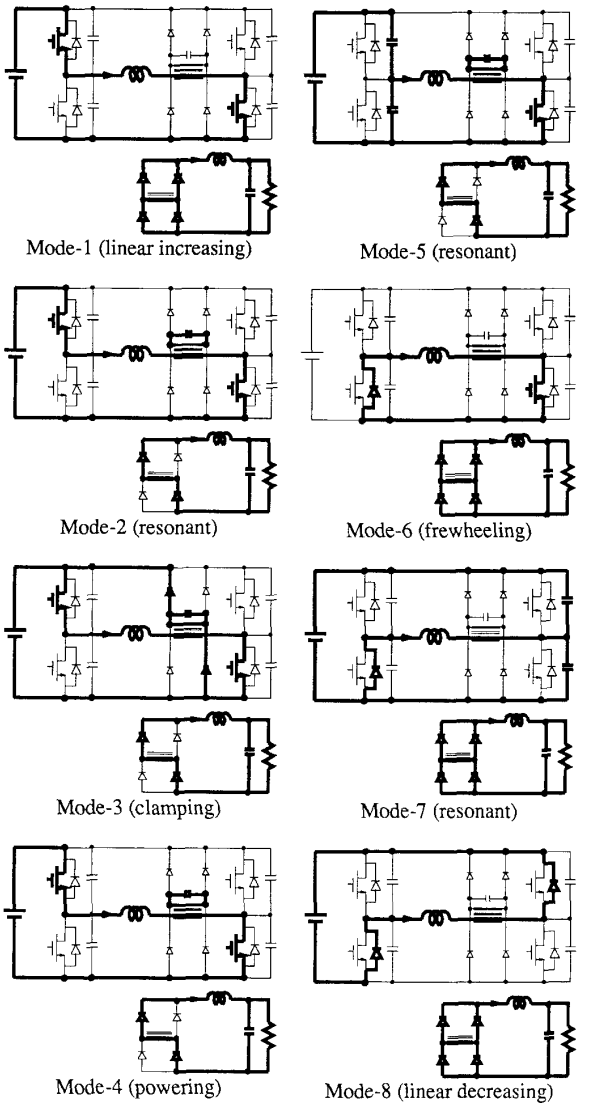

Fig. 7 Topological mode diagrams of proposed converter.

Since $V_S(1-a)/Z_{rr}$ is usually designed much smaller than I_O, the resonant inductor current i_{Lr} is limited to the output current I_O which varies smoothly. The capacitor voltage V_{Crr} resonate having small amount of energy and finally decays to $V_S-(V_S-V_O)L_r/(L_r+L_O)$ which is determined by the divided voltage between the series-connected L_r and L_O. After a finite time-interval T_{on}, switch S_1 is turned off under zero voltage switching condition.

(V). Mode 5 (*resonant*) : By turning off the switch S1, the current path is altered from switch S1 to capacitors C1 and C3. The series-connected resonant and filter inductors are partially resonant with the capacitors C_1, C_3, C_{rr} and the capacitor voltage v_{C3} begins to decrease from the source voltage, that is,

$$V_{C3}=V_S-\frac{I_O}{2C_r+C_{rr}/a^2}(t+\frac{C_{rr}}{2C_ra^2\omega_p}\sin\omega_p t)$$

$$+\frac{(V_S-V_O)L_r}{2C_r\omega_p Z_p(L_O+L_r)}(1-\cos\omega_p t) \quad (16)$$

$$V_{rr}=\frac{1}{a}[V_S-\frac{L_r(V_S-V_O)}{L_O+L_r}-\frac{I_O(t+1/\omega_p\sin\omega_p t)}{2C_r+C_{rr}/a^2}$$

$$+\frac{(V_S-V_O)L_r}{C_{rr}/a^2\omega_p Z_P(L_O+L_r)}(1-\cos\omega_p t)] \quad (17)$$

$$\omega_p=\sqrt{\frac{2C_r+C_{rr}/a^2}{2C_rC_{rr}/a^2L_r}} \quad (18)$$

$$Z_p=\sqrt{\frac{L_r(2C_r+C_{rr}/a^2)}{2C_rC_{rr}/a^2}} \quad . \quad (19)$$

When the capacitor voltage v_{C3} reaches zero, the diode D3 begins to conduct and this mode ends (It is assumed that V_{C3} and V_{Crr} reach zero simultaneously despite of small difference. If the difference becomes large one more mode should be added). In particular, the capacitor current i_{C3} flows only during this short interval and the VAR ratings of the resonant capacitor are significantly reduced compared with those of the resonant type converter.

(VI). Mode 6 (*freewheeling*) : This mode corresponds to the freewheeling mode of the conventional PWM DC/DC converter. During the above four modes the resonant inductor and the output filter inductor are effectively series-connected. Starting from this mode, two inductors are effectively decoupled through short-circuit of the output bridge diodes as shown in Fig. 3(b). The two inductor currents decrease linearly as

$$i_{Lr}(t)=i_{Lr}(t_5)-\frac{V_{D.on}+V_{FET.on}}{L_r}t, \quad (20)$$

$$I_O(t)=I_O(t_5)-\frac{V_O}{L_O}t. \quad (21)$$

At proper time t_3, switch S4 is turned off under zero voltage switching condition.

(VII). Mode 7 (*resonant*) : The resonant inductor current i_{Lr} discharges and charges the capacitors C2 and C4 through resonant operation until the capacitor voltage v_{C2} decreases to zero from supply voltage.

(VIII). Mode 8 (*linear decreasing*) : When the capacitor voltage reaches zero, diode D2 begin to conduct and the resonant inductor current i_{Lr} decreases linearly and rapidly by the supply voltage :

$$i_{Lr}(t)=i_{Lr}(t_7)-\frac{V_s}{L_r}t. \quad (22)$$

The pre-triggering signals of the switches S2 and S3 are initiated here in order to ensure zero voltage switching condition at the start of the next cycle. When the resonant inductor current reaches zero, the diodes D2 and D3 are turned off and the switches S2 and S3 are turned on.

VI. ANALYSIS OF THE PROPOSED CONVERTER

The converter is designed for the maximum power $P_{o.max}$ = 1.5 [kW] at 100 [kHz] of operating frequency. The parameter values are L_r = 4 [μH], L_o = 25 [μH], $C_r(C_1-C_4)$ = 3 [nF] and C_{rr} = 1 [nF]. The proposed converter can be modeled as the equivalent circuit shown in Fig. 8 to derive DC conversion-ratio characteristics. The equivalent voltage V_{eq} of the AC resonant

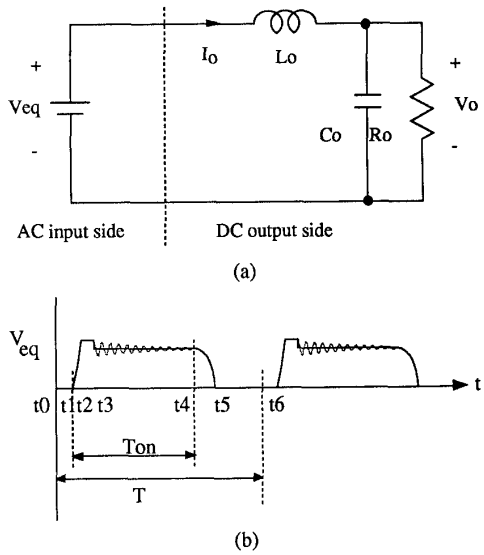

Fig. 8 DC conversion-ratio derivation (a) equivalent circuit, (b) equivalent waveform V_{eq} referred to the DC output side.

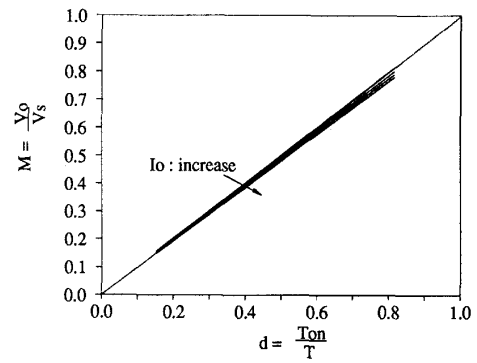

Fig. 9 DC conversion-ratio characteristics of the proposed converter for several values of I_O = 5, 10, 15, 20 [A].

input side referred to DC output side is as follows :

$$V_{eq}=\begin{cases} aV_{Crr} \quad (V_{Crr} : Eq.(10)) & (t_1<t<t_2) \quad (23)\\ aV_S & (t_2<t<t_3) \quad (24)\\ V_S-\frac{L_r}{L_O+L_r}(V_S-V_O) & (t_3<t<t_4) \quad (25)\\ aV_{rr} \quad (V_{rr} : Eq.(17)) & (t_4<t<t_5) \quad . \quad (26)\end{cases}$$

The average output voltage V_O can be calculated to be

$$V_O=\int_{t_0}^{t_6}V_{eq}\,dt \quad . \quad (27)$$

Then the DC conversion-ratio M and and the duty ratio d are defined as

$$M=\frac{V_o}{V_s} \quad (28)$$

$$d=\frac{T_{on}}{T} \quad . \quad (29)$$

From the above equations, the DC conversion characteristics can be obtained. The DC characteristics are linear and almost load-

independent as shown in Fig. 9, which are better than those of any other similar converters. It deviates slightly from the characteristic curve (dotted line) of the PWM DC/DC converter depending on the load variations. The deviation arises from a little voltage drop across the resonant inductor.

Fig. 10 shows normalized device voltage stresses of the proposed converter, comparing with those of several typical converters. The voltage stresses of the devices and components are always limited to the supply voltage V_S like switched mode PWM converter despite of the variations of load condition.

Fig. 11 shows normalized device current stresses of the proposed converter together with three other typical converters. The current stresses are also clamped to the output current I_O. The current stresses of the proposed converter are almost the same as those of switched mode PWM converter and much lower than those of any other converters such as the series-resonant converter, resonant pole type converter and ZCS quasi-resonant converter.

It should also be stressed that the auxiliary windings and the bridge diodes are connected to the supply side but not to the output capacitor side. By doing so clamping operation is always guaranteed even if the supply voltage varies with large ripple because the clamp voltage will also follow the supply voltage variation. For comparison, if the auxiliary winding and the bridge diodes are connected to the output capacitor side, the clamping operation will not work properly when the supply voltage varies in a wide range because the output capacitor voltage and thus the clamp voltage will remain almost constant through the output voltage regulation. If the clamp voltage is fixed, shoot-through phenomenon may occur through the auxiliary winding and the bridge diodes to the output side when the supply voltage increases above a certain limit. In the proposed converter, the large voltage spikes of output diodes can simply and effectively be limited to $(n_1/n_3)V_S$ (almost $1<n_1/n_3<1.1$). Fig. 12 shows the magnified waveform considering the reverse-recovery effect of the output diodes. The suppressed ripple voltage ΔV, which would be very large in the pre-proposed type, can be found to be

$$\Delta V = V_S[a - \frac{L_O}{L_r + L_o}] - V_O \frac{L_r}{L_r + L_O}. \quad (30)$$

Fig. 13 shows the normalized ripple voltage $\Delta V/V_S$ for various L_r/L_o values. The normalized ripple voltage is very small and slightly dependent on V_O/V_S, and can be considered to be

$$\Delta V = kV_S \quad (k<0.2). \quad (31)$$

Consequently the large voltage spikes of the output diodes is adaptively and effectively limited by the auxiliary clamp circuit.

The auxiliary bridge diodes carry a triangular waveform current only during the clamping operation. The current waveform i_{Da1}, i_{Da4} can be expressed as

$$i_{Da1}(i_{Da4}) = [V_S(1-a) - 2V_{FET.on} - 2aV_{D.on}]^* t + a\sqrt{I_{RP}^2 + (V_s/Z_{rr})^2} \quad (32)$$

Then the average power ratings of the auxiliary clamp circuit can be calculated as

$$P_{aux.} = \frac{V_s L_r [I_{RP}^2 + (V_s/Z_{rr})^2]}{2aT_s[V_S(1-a) - 2V_{FET.on} - 2aV_{D.on}]} \quad (33)$$

Fig. 14 shows the average auxiliary power $P_{aux.}$ for various turn-ratio a($=n_1/n_3$) values, indicating that power rating of auxiliary clamp circuit is influenced by the load current but low enough.

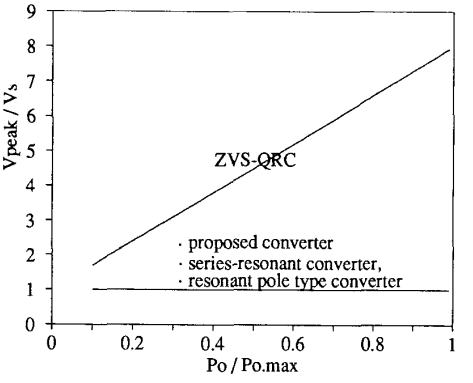

Fig. 10 Comparison of peak voltgae stresses of four different converters.

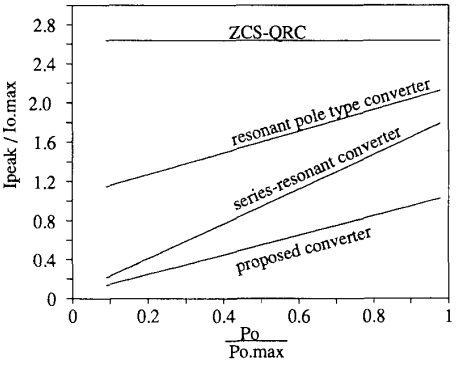

Fig. 11 Comparison of peak current stresses of four different converters.

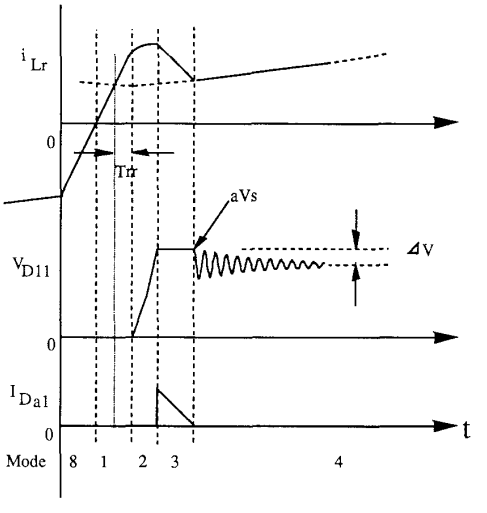

Fig. 12 The magnified waveforms of proposed converter including reverse recovery effect of output diodes (T_{rr} : reverse recovery interval).

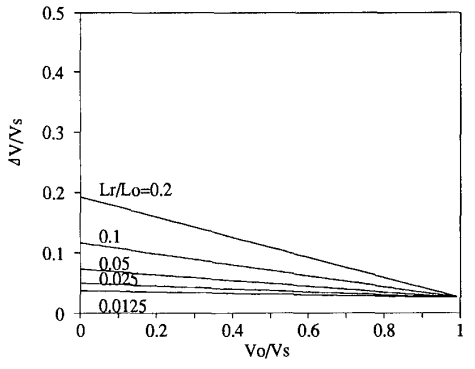

Fig. 13 Normalized ripple voltage $\Delta V/V_S$ .vs. V_O/V_S for several Lr/Lo values at n_1/n_3 =1.025.

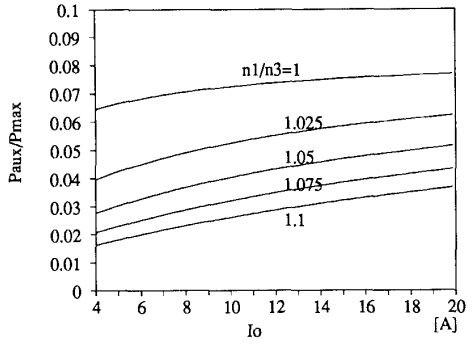

Fig. 14 Normalized handling power P_{aux} of auxiliary circuit for several transformer turn-ratio values.

VII. CONCLUSION

A new zero-voltage-switching constant frequency PWM DC/DC converter is proposed. The proposed converter has low VA ratings of the devices and components, constant switching frequency operation and almost linear and load-independent DC conversion-ratio characteristics. The voltage and current stresses are low and always limited to the supply voltage V_S and the output current I_O, respectively. Finally, the proposed converter has low switching loss due to zero voltage switching for all of the devices including output rectifier diodes and thus can operate at high frequency. The features of the proposed converter are summarized as follows:

1) linear and almost load-independent DC conversion-ratio characteristic,
2) constant frequency PWM operation,
3) low voltage and current stress,
4) low switching loss,
5) simple control,
6) low VAR ratings of the resonant elements,
7) no reverse recovery problem.

REFERENCES

[1] R. L. Steigerward, " High frequency resonant transistor dc-dc converter , " IEEE Trans. Ind. Electron., vol. IE-31, No. 2, pp181-192, May 1984.

[2] F. C. Schwarz, " An improved method of resonant current pulse modulation for power converters, " IEEE Trans. Ind. Electron. Con. Instr., vol. IECI-23, No. 2, pp133-141, May 1976.

[3] K. Liu, R. Oruganti and F. C. Lee, " Quasi-resonant converters topologies and characteristics, " IEEE Trans. Pow. Electron., vol. PE-2, No. 1, pp62-71, Jan. 1987.

[4] R. W. De Doncker, D. M. Divan and M. H. Kheraluwala, "A Three-Phase Soft-Switched High Power Density DC/DC converter For High Power Applications", IEEE IAS Annu. Meeting Rec., 1988, pp. 796-804

[5] E. C. Nho and G. H. Cho, " A New High Performance zero-voltage zero-current mixed mode switching DC/DC converter, " IEEE-PESC Rec., 1989, PP. 902-908.